# Regime Analysis with Numerical Modelling of Wave Dynamics and Determination of Potential Flood Zones in Chancay Bay, Peru

Jose Soto[a], Emanuel Guzman[b] and Carmela Ramos[c]
*Facultad y Escuela de Ingeniería Civil, Universidad Peruana de Ciencias Aplicadas, Av. Prolongación Primavera 2390, Santiago de Surco, Lima, Peru*

Keywords: Chancay Bay, Wave Dynamics, Dihidronav, Delft3d Wave, Wave Modeling.

Abstract: The wave dynamics in Chancay Bay is represented by the Delft3D numerical model, whose application is referred to the propagation and calibration of the waves in the WAVE module through the Copernicus ERA5 database and comparison with field measurements of the hologram of the Directorate of Hydrography and Navigation. (DIHIDRONAV) for medium and maximum regime conditions, in order to determine the Run Up of waves in areas of human development with the Van Der Meer and Stem methodology. In this sense, the topography of the ALOS PALSAR sentinel was extracted to determine the flood zones within the coast, whose representation is given by the length and height of the wave reached.

## 1 INTRODUCTION

The study of wave dynamics in coastal areas is carried out through numerical models whose interest is multipurpose decision-making management. This is why characterizing the waves in coastal areas is a mandatory task, but one that is frequently limited due to its complexity of execution and lack of information from field and/or satellite measurements.

This is reflected in many investigations that, through statistical adjustments, calibrate the numerical models until a reliable approximation is obtained through data collection and is compared with in situ measurements to be adjusted using correction models (Wang et al., 2022). On the other hand, within coastal studies, understanding the interactions of waves, tides and currents in coastal regions has become a fundamental aspect to develop best practices in numerical modeling methodology (Pinault et al., 2020) (Prakash et al., 2021). Likewise, there are different quasi-3D models, of which Delft3D, Mike21, TELEMAC and SWAN stand out. These 4 models are commonly used by researchers to perform analysis of wave behavior. Of those mentioned, Delft3D presents good results, since this software allows the coupling of modules that allow establishing an expansion in the analysis and reducing or optimizing modeling time (Villagrán et al., 2022). Therefore, it is feasible to establish a before and after that allows generating warnings or effective solutions to coastal hazards (Leach et al., 2021).

Therefore, in this article the wave characterization will be carried out with the medium regime method of Chancay Bay, Figure 1, for three numerical modeling scenarios in the Delft3D software using satellite information from the current year and nautical chart of Chancay Bay in its latest version, as well as data from Copernicus ERA5 over a period of 30 years and field measurements requested from the Directorate of Hydrography and Navigation (DIHIDRONAV) in its latest version.

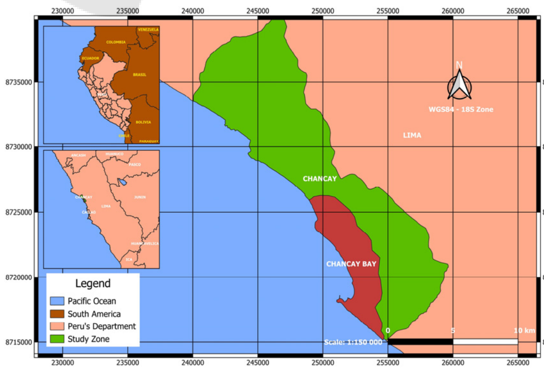


Figure 1: Study Zone of Chancay.

[a] https://orcid.org/0009-0002-6315-0228
[b] https://orcid.org/0000-0001-8381-4509
[c] https://orcid.org/0000-0002-4269-2944



Soto, J., Guzman, E. and Ramos, C.
Regime Analysis with Numerical Modelling of Wave Dynamics and Determination of Potential Flood Zones in Chancay Bay, Peru.
DOI: 10.5220/0012631700003696

In *Proceedings of the 10th International Conference on Geographical Information Systems Theory, Applications and Management (GISTAM 2024)*, pages 51-61
ISBN: 978-989-758-694-1; ISSN: 2184-500X

Likewise, this article aims to determine the potential flood zones through a numerical model and compare its results with data taken in the field, as well as a tentative location of coastal structures.

# 2 METHODOLOGY

## 2.1 Tools

Delft3D is a numerical modeling software widely used in coastal zone research, since very good results are obtained, and it is easy to acquire through educational licenses valid for up to one year. Likewise, Delft3D has the WAVE module which simulates the evolution of waves generated by wind in coastal areas (Deltares, 2023). This module models the propagation of waves and waves generated by wind, which in turn considers the effects generated by wave diffraction and refraction. As input values, the bathymetry of the area in UTM coordinates and height, period and wave direction data are assigned.

## 2.2 Materials

To carry out numerical modeling in the medium regime, in situ information from DIHIDRONAV for the years 2008 and 2009 from the ADCP Nortek AS (R) has been used, as well as oceanographic data from Copernicus ERA 5.

In the case of bathymetric information, the nautical chart of Chancay Bay was acquired in .TIF format from DIHIDRONAV and updated satellite information of the coastline from Google Earth.

## 2.3 Method

The mean regime method is used to statistically classify the highest and average values of a time series for each cardinal direction of wave propagation, Figure 2. This is possible by programming in RStudio and MATLAB. As it is encrypted information, the data is extracted in RStudio in .xlsx format and in MATLAB the classification is provided as a result with the configuration indicated in the code.

## 2.4 Data Used

The nautical chart of Chancay Bay is digitized the depths and coastline, while the current satellite information is digitized the coastline. Likewise, with the data collected for a period of more than 30 years of Copernicus ERA5, the extraction and classification

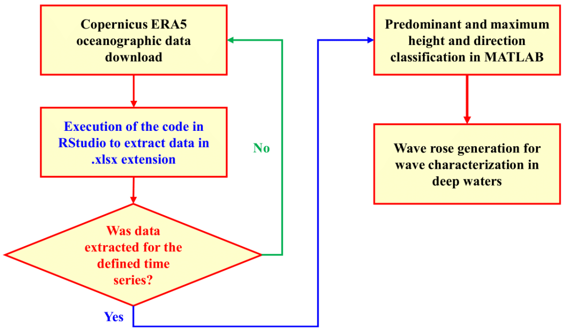


Figure 2: Processing flow diagram and obtaining medium regime classification.

procedure are carried out with the medium regime method. On the other hand, the ADCP's in situ data was already classified. With the information available, three modelling cases are classified in different conditions for Chancay Bay, as a result, they are the following.

The first case is a regime analysis for a wave of more than 30 years with bathymetric data from the nautical chart of Chancay Bay.

Then, a regime analysis for a wave from the years 2008 and 2009 with bathymetric data from the Chancay nautical chart.

Finally, a regime analysis for a wave of more than 30 years with satellite bathymetric data to date.

## 2.5 Wave Characterization in Deep Waters

The general characteristics such as cardinal direction and wave height in shallow waters, Figure 3, that predominate in Chancay Bay are coming from the south with an average height of between 1.3 and 2.1

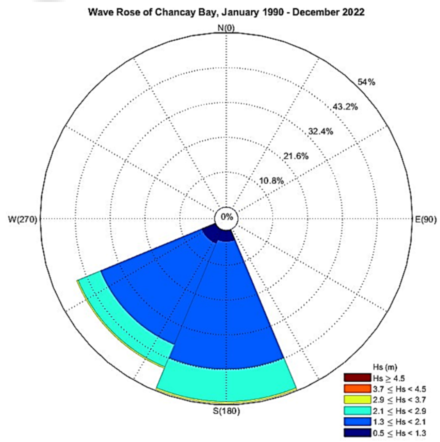


Figure 3: Wave rose in shallow water of Chancay bay (S11°34'17" W77°16'1.99").

meters, and less frequently, but of greater height between 2.9 and 3.7 meters. There are also wave heights of between 3.7 to 4.5 meters and higher, which are not visible due to their low frequency, but are not non-existent.

Now that the general characteristics are known, in Table 1, the classified wave data for the 1st and 3rd modeling case is observed, while in Table 2, the classified wave data for the 2nd modeling case is observed. In both, the average and maximum cases are handled for each cardinal direction.

Table 1: Average regime for wave data for a period of more than 30 years from Copernicus ERA5.

| Case | Dir | Hs (m) | Tp (s) | Case | Dir | Hs (m) | Tp (s) |
|---|---|---|---|---|---|---|---|
| 1 | WSW | 1.54 | 10.82 | 5 | SW | 1.69 | 11.12 |
| 2 | | 1.97 | 12.00 | 6 | | 3.48 | 16.04 |
| 3 | S | 1.92 | 8.66 | 7 | SSW | 1.76 | 10.12 |
| 4 | | 3.71 | 13.21 | 8 | | 4.23 | 16.09 |

Table 2: Average regime for wave data from the DIHIDRONAV ADCP for the years 2008 and 2009.

| Case | Dir | Hs (m) | Tp (s) |
|---|---|---|---|
| 1 | S | 1.92 | 8.81 |
| 2 | | 2.66 | 13.21 |
| 3 | SW | 1.71 | 10.89 |
| 4 | | 3.06 | 14.13 |
| 5 | SSW | 1.69 | 9.99 |
| 6 | | 2.83 | 14.46 |

## 2.6 Numerical Modeling

The Delft3D model operates within a discrete domain, defining a particular calculation region through a computational mesh. The RGFGRID module prepares this mesh, and the QUICKIN module uses triangular interpolation to determine depths based on digitized bathymetry.

Likewise, Figure 4 shows the computational domain for numerical modelling. On the other hand, Table 3 presents the geometric characteristics of said domain.

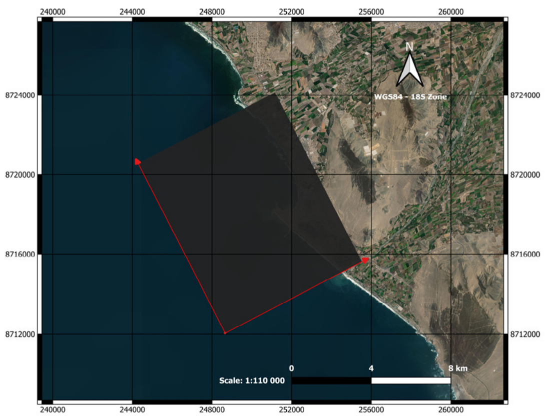


Figure 4: Computational mesh calculation in Chancay Bay.

Table 3: Average regime for wave data from the DIHIDRONAV ADCP for the years 2008 and 2009.

| Shallow waters | |
|---|---|
| **Computational grid** | |
| **Long (km)** | 9.53 |
| **Width (km)** | 7.72 |
| **dx (m)** | 15.00 |
| **dy (m)** | 20.00 |
| **Angle (°)** | 24.00 |

Finally, in the WAVE module, the input values of height, period, and direction from Tables 1 and 2 are entered according to the direction of wave propagation.

# 3 RESULTS AND DISCUSSIONS

Of the three modeling cases, the first case, according to Table 1, gives 8 results for the west-southwest, south, southwest, and south-southwest directions in its predominant and maximum conditions. Of which, the maxims will be highlighted, as they are most relevant to the knowledge of potential flood zones.

Figure 5, Figure 6, Figure 7 and Figure 8 show the results for the maximum wave conditions of Chancay Bay from the first modeling case. For the west-southwest direction the following result was obtained.

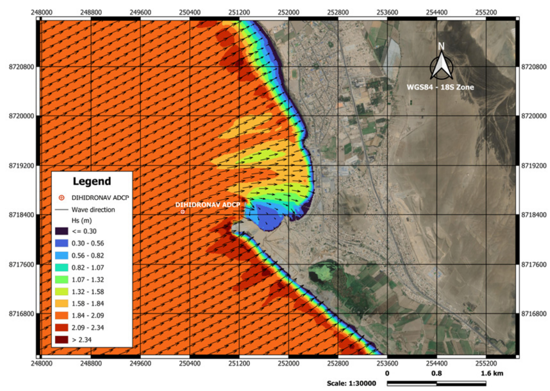


Figure 5: Maximum condition in west-southwest direction in Chancay Bay.

For the south direction in maximum wave conditions of Chancay Bay.

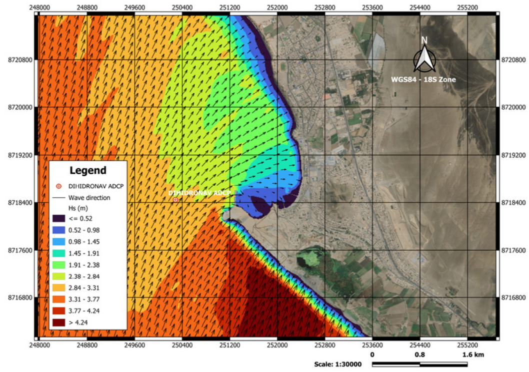


Figure 6: Maximum condition in south direction in Chancay Bay.

Likewise, for the southwest direction in maximum wave conditions of Chancay Bay.

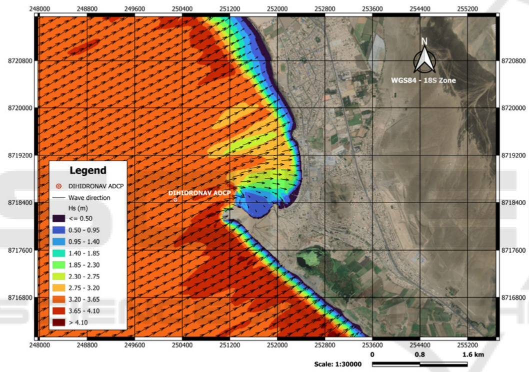


Figure 7: Maximum condition in southwest direction in Chancay Bay.

Also, for the south-southwest direction in maximum wave conditions in Chancay Bay.

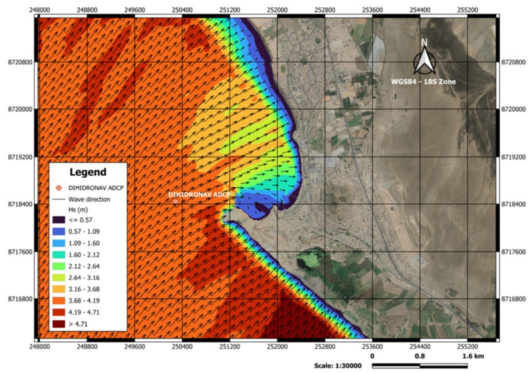


Figure 8: Maximum condition in a south-southwest direction in Chancay Bay.

The second case, according to Table 2, gives 6 results for the south, southwest, south-southwest directions. Of which, the maxims will be highlighted; Figure 9, Figure 10 and Figure 11 for what was previously said, to know the potential flooding zones.

Then, for the south direction in maximum wave conditions of Chancay Bay, the following result was obtained.

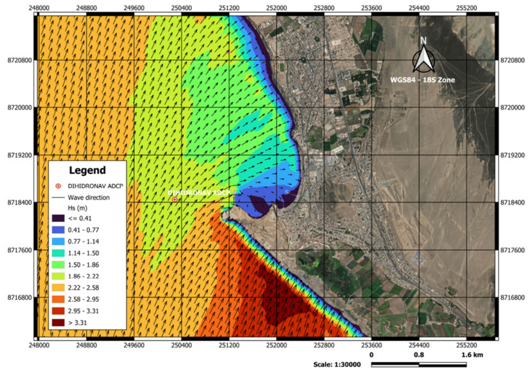


Figure 9: Maximum condition in a southerly direction in Chancay Bay.

Additionally, for the southwest direction in maximum wave conditions of Chancay Bay.

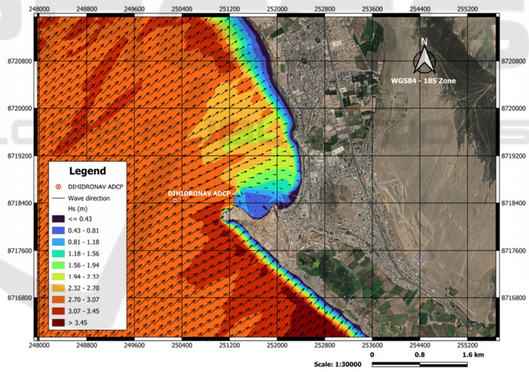


Figure 10: Maximum condition in southwest direction in Chancay Bay.

Also, for the south-southwest direction in maximum wave conditions of Chancay Bay.

This second modeling case, since it does not have an updated bathymetry and current in situ wave data, except for the ADCP whose measurement is valid until 2009, which can be validated through ERA5 data from 2008 to 2009, is calibrated in function of the bottom friction coefficient of the model until obtaining approximate results.

Based on the results of the second modeling case, the wave Run Up is estimated for three points in the

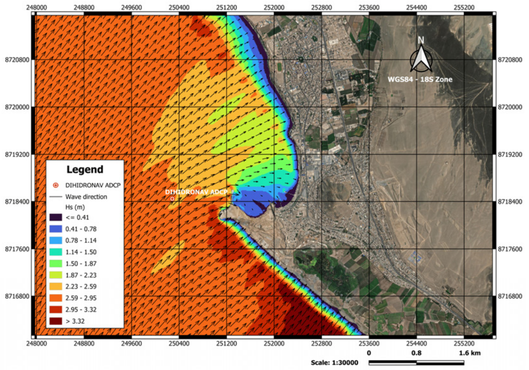


Figure 11: Maximum condition in a south-southwest direction in Chancay Bay.

area that are within or close to the surf zones. These areas were chosen because they have the highest concentration of human activity, such as commerce and fishing. Of the analysis points mentioned, only the first three that are presented in Figure 12 and Figure 13 are considered.

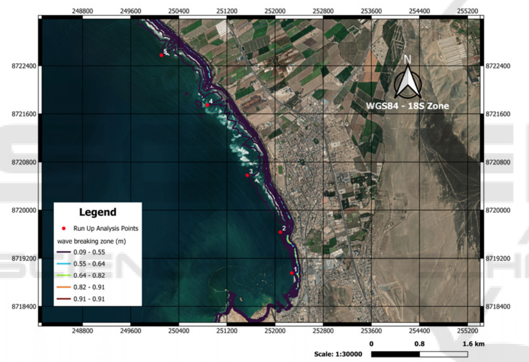


Figure 12: Analysis points to estimate the Run Up of the wave in the south direction.

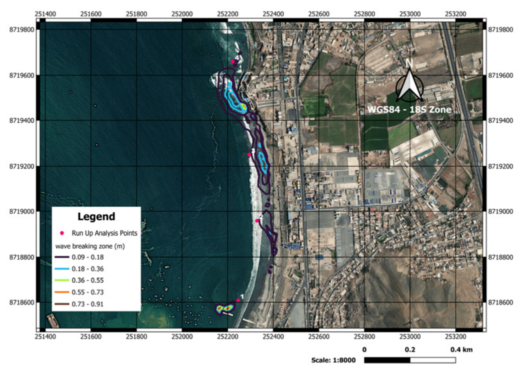


Figure 13: Analysis points to estimate the Run Up of the wave in the south-southwest direction.

The following Table 4 displays the parameters obtained for said calculation, which are a function of the bathymetry depth, height, and wave distance at said point with respect to the coast from the surf zone, which can be seen in Figure 12-13 and summarized in Table 4.

Table 4: Summary of distances, depth, and heights of the points of interest of the Run Up calculation under maximum conditions.

| Dir | Poin | Model Distance (m) | Model Depth (m) | Model Hs (m) | Regime Analysis Hs (m) | Regime Analysis Tp (s) |
|---|---|---|---|---|---|---|
| S | 1 | 362.40 | 2.90 | 1.88 | 2.66 | 13.21 |
| | 2 | 217.71 | 2.90 | 1.70 | 2.66 | 13.21 |
| | 3 | 135.42 | 2.90 | 1.25 | 2.66 | 13.21 |
| SW | - | - | - | - | - | - |
| SSW | 1 | 80.90 | 1.40 | 0.46 | 2.83 | 14.46 |
| | 2 | 78.00 | 1.40 | 0.85 | 2.83 | 14.46 |
| | 3 | 84.02 | 1.40 | 0.74 | 2.83 | 14.46 |

Finally, the third case, based on Table 1, gives, like the first modeling scenario, 8 results for the west-southwest, south, southwest, and south-southwest directions. This will also highlight the results of the maximum conditions, as they are more relevant to the knowledge of potential flood zones.

The difference between the first and third modeling cases is the change in the bathymetry and coastline used. The first specifies the use of the nautical chart until its last update, which dates to 2005, while the third uses the same bathymetry of the nautical chart with the current coastline provided by Google Earth.

In Figure 14, Figure 15, Figure 16, and Figure 17 the results of the third case of numerical modeling for Chancay Bay in maximum conditions will be seen.

So, for the west-southwest direction in maximum wave conditions of Chancay Bay.

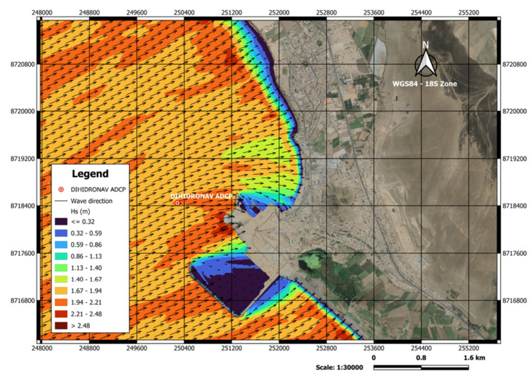


Figure 14: Maximum condition in west-southwest direction in Chancay Bay.

For the south direction in maximum wave conditions of Chancay Bay.

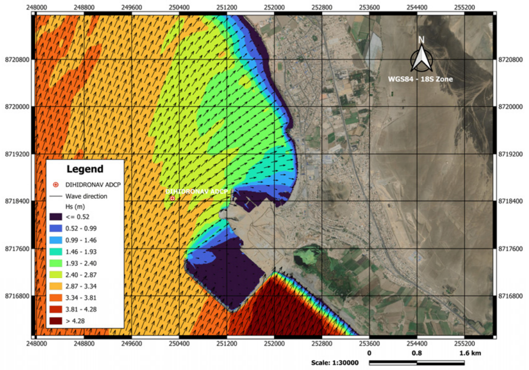


Figure 15: Maximum condition in a southerly direction in Chancay Bay.

For the southwest direction in maximum wave conditions of Chancay Bay.

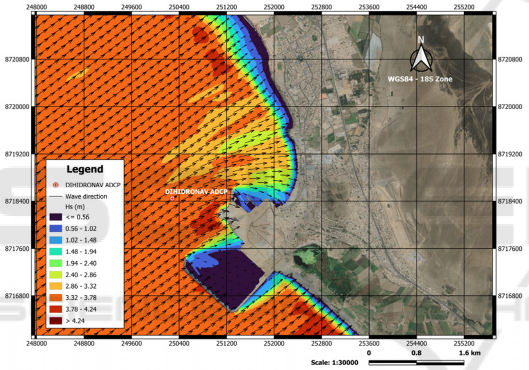


Figure 16: Maximum condition in southwest direction in Chancay Bay.

For the south-southwest direction in maximum wave conditions of Chancay Bay.

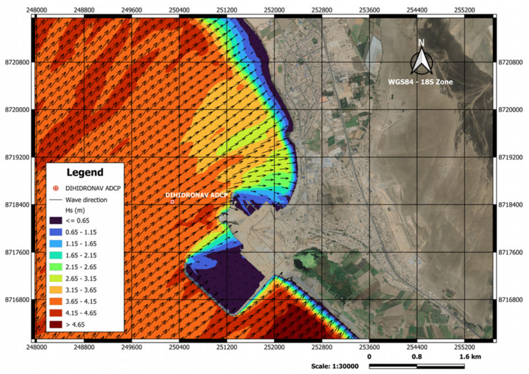


Figure 17: Maximum condition in a south-southwest direction in Chancay Bay.

Although the results presented are from scenarios with conditions that vary the bathymetry, coastline and wave reanalysis of ERA5, the advantages and/or disadvantages of these range from modeling in context to not having many in situ measurements. Table 5 presents the comparison between these modeling scenarios according to the mentioned conditions.

Table 5: Summary of the characteristics and usefulness that it would have in a future numerical modeling of Chancay Bay.

| **Desc** | **Case 1** | **Case 2** | **Case 3** |
|---|---|---|---|
| **Bathymetry** | Nautical chart outdated compared to the year in which this research was carried out. | Nautical chart outdated compared to the year in which this research was carried out. | Outdated nautical chart, but with an updated coastline compared to the year in which this research was carried out. |
| **In situ measurements** | Outdated in situ measurement s compared to the year in which this research was carried out. | In situ measurements updated with the bathymetric information of the model made. | In situ measurements outdated with respect to the year in which this research was carried out. |
| **Coastal line** | Coastline outdated as of the year this research was conducted. | Coastline updated to the year in which the bathymetric and measurement information of the model carried out was collected. | Coastline updated to the year this research was carried out. |
| **Utility** | It serves as a model for validation only if satellite images from recent years are available. | It serves as a model for validation only if satellite images from recent years are available. | It serves as a model for validation only if satellite images from recent years are available. |

In this sense, the advantages of carrying out a medium regime analysis in Chancay Bay can be traced back to the validation of future scenarios with the use of primary information available to date. However, this limits the information regarding the timing of the waves, since in recent years Peru has presented climatic phenomena such as “Fenómeno El Niño Costero” and “Ciclón Yaku” that alter the wave regime. Therefore, future modeling would require greater computational scope. That is, cover larger areas for wave propagation in areas that do have information from later years.

With emphasis on the aforementioned idea, in the country of Peru, research titled "Simulación de transporte de sedimentos en la bahía Ferrol, Chimbote" was carried out, whose numerical model was based on the concept of selecting the most representative wave cases, validation of the numerical model with DIHIDRONAV holograph measurements and future prediction for the selected conditions (Ramos, 2017). As a result of its calibration and validation, it used the same energy dissipation calibration parameters to obtain a predictive model for a time of 20 years in the future.

# 4 ANALYSYS OF RESULTS

For the first modeling case, the following Delft3D results were obtained referring to the wave height in Table 6.

Table 6: Summary of results obtained from the medium regime and ADCP of the first modeling case.

| Dir | Measurement | Predominant Condition | | Maximum Condition | |
|---|---|---|---|---|---|
| | | Hs (m) | Tp (s) | Hs (m) | Tp (s) |
| WSW | In Situ | 1.30 | 12.60 | 2.10 | 17.30 |
| | Delft3D | 1.49 | - | 1.96 | - |
| | **Error (%)** | 14.62 | - | 6.67 | - |
| S | In Situ | 1.30 | 12.60 | 2.10 | 17.30 |
| | Delft3D | 1.50 | - | 2.85 | - |
| | **Error (%)** | 15.38 | - | 35.71 | - |
| SW | In Situ | 1.30 | 12.60 | 2.10 | 17.30 |
| | Delft3D | 1.52 | - | 3.54 | - |
| | **Error (%)** | 16.92 | - | 68.57 | - |
| SSW | In Situ | 1.30 | 12.60 | 2.10 | 17.30 |
| | Delft3D | 1.44 | - | 3.90 | - |
| | **Error (%)** | 10.77 | - | 85.71 | - |

As can be seen, there are wave heights that are above the ADCP in situ measurement data, and some are even higher than 50% of the real value, which are the southwest and south-southwest directions.

On the other hand, in the second modeling case, the following Delft3D results were obtained referring to the wave height in Table 7.

Table 7: Summary of results obtained from the medium regime and ADCP of the second modeling case.

| Dir | Measurement | Predominant Condition | | Maximum Condition | |
|---|---|---|---|---|---|
| | | Hs (m) | Tp (s) | Hs (m) | Tp (s) |
| S | In Situ | 1.30 | 12.60 | 2.10 | 17.30 |
| | Delft3D | 1.50 | - | 2.05 | - |
| | **Error (%)** | **15.38** | - | **2.38** | - |
| SW | In Situ | 1.30 | 12.60 | 2.10 | 17.30 |
| | Delft3D | 1.53 | - | 2.92 | - |
| | **Error (%)** | **17.69** | - | **39.05** | - |
| SSW | In Situ | 1.30 | 12.60 | 2.10 | 17.30 |
| | Delft3D | 1.38 | - | 2.60 | - |
| | **Error (%)** | **6.15** | - | **23.8** | - |

As can be seen, the wave heights obtained by the Delft3D model are very close to the in-situ measurement. Except for the southwest and south-southwest directions that exceed in a range of 20-40%.

Likewise, in the third modeling scenario, the following Delft3D results were obtained, also referring to wave height, Table 7.

Table 8: Summary of results obtained from the medium regime and ADCP of the third modeling case.

| Dir | Measurement | Predominant Condition | | Maximum Condition | |
|---|---|---|---|---|---|
| | | Hs (m) | Tp (s) | Hs (m) | Tp (s) |
| WSW | In Situ | 1.30 | 12.60 | 2.10 | 17.30 |
| | Delft3D | 1.47 | - | 1.95 | - |
| | **Error (%)** | **13.08** | - | **7.14** | - |
| S | In Situ | 1.30 | 12.60 | 2.10 | 17.30 |
| | Delft3D | 1.47 | - | 2.79 | - |
| | **Error (%)** | **13.08** | - | **32.86** | - |
| SW | In Situ | 1.30 | 12.60 | 2.10 | 17.30 |
| | Delft3D | 1.50 | - | 3.52 | - |
| | **Error (%)** | **15.38** | - | **67.62** | - |
| SSW | In Situ | 1.30 | 12.60 | 2.10 | 17.30 |
| | Delft3D | 1.42 | - | 3.88 | - |
| | **Error (%)** | **9.23** | - | **84.76** | - |

Based on Table 6, Table 7 and Table 8, exceedance patterns are observed with respect to the wave height measured by the ADCP in the southwest and south-southwest directions, which are greater than 50% with respect to the actual measurement value.

Although the 3 modeling cases can be calibrated in the same Delft3d WAVE model, it was decided to work only with the second case, since it is the one that works with all the most current data officially, both bathymetry, measurement, and line coast.

Therefore, the Run Up calculation based on Table IV and the methodology of Van Der Meer and Stam gave the following results, Table 9, after having done the calibration.

Table 9: Wave Run Up calculation with the Van Der Meer and Stam formulation for maximum wave conditions considering the tide level.

| Method | S | | SW | | SSW | |
|---|---|---|---|---|---|---|
| Van Der Meer y Stam (1992) | Ru 10% (m) = | 3.70 | Ru 10% (m) = | - | Ru 10% (m) = | 1.60 |
| | Ru 5% (m) = | 4.10 | Ru 5% (m) = | - | Ru 5% (m) = | 1.70 |
| | Ru 2% (m) = | 4.70 | Ru 2% (m) = | - | Ru 2% (m) = | 1.90 |
| | Ru 10% (m) = | 3.40 | Ru 10% (m) = | - | Ru 10% (m) = | 1.20 |
| | Ru 5% (m) = | 3.80 | Ru 5% (m) = | - | Ru 5% (m) = | 2.40 |
| | Ru 2% (m) = | 4.30 | Ru 2% (m) = | - | Ru 2% (m) = | 2.60 |
| | Ru 10% (m) = | 2.80 | Ru 10% (m) = | - | Ru 10% (m) = | 2.00 |
| | Ru 5% (m) = | 3.10 | Ru 5% (m) = | - | Ru 5% (m) = | 2.20 |
| | Ru 2% (m) = | 3.40 | Ru 2% (m) = | - | Ru 2% (m) = | 2.40 |

In this Table 9, the wave Run Ups were obtained for the probability of occurrence of 10%, 5% and 2% for the 3 selected points in the south and south-southwest directions. In the southwest there were no important surf zones, so they are not considered. Of these, the wave heights with the highest percentage represent heights in normal conditions, while a lower percentage represents heights in maximum conditions.

Additionally, the tide level is considered, the difference between the highest and lowest level being the result of this, which is added to the Run Up obtained, which by polling DIHIDRONAV tide tables gives a value of 0.97 m.

The south direction presents higher waves compared to the south-southwest direction, despite this both represent a danger to human activity in coastal areas, since the heights can exceed terrain levels greater than 4 meters and a large part of the shops or points of port activity in the area are located near the coastline whose elevation is 0 meters.

The wave heights obtained do not mean that they will enter the coastal zone maintaining the same height in magnitude, these will be reduced until they reach or exceed the terrain levels according to the wave height obtained, but with minimum wave heights that may be called sheets of water. However, its height may be minimal, but its extension within the coastal zone may be wide. This suggests that the impact of the wave alone should not be underestimated because of its apparently small size.

In that sense, flood zones are estimated through interpolation between contour lines of the Alos Palsar DEM and elevations from Google Earth since the elevations of the DEM are over scales of the real height.

Table 10 shows the summary of the interpolation carried out, from which a proportional ratio was detected between the Google Earth elevations and the Alos Palsar DEM.

Table 10: Summary of the elevation interpolation process between Alos Palsar and Google Earth.

| INTERPOLATION TO ALOS PALSAR | | | |
|---|---|---|---|
| Google Earth | | DEM Alos Palsar | |
| Elevation (m) | 1.00 | Elevation (m) | 21.00 |
| | 2.00 | | 23.00 |
| | 3.00 | | 25.00 |
| | 4.00 | | 27.00 |
| | 5.00 | | 29.00 |
| | 6.00 | | 31.00 |

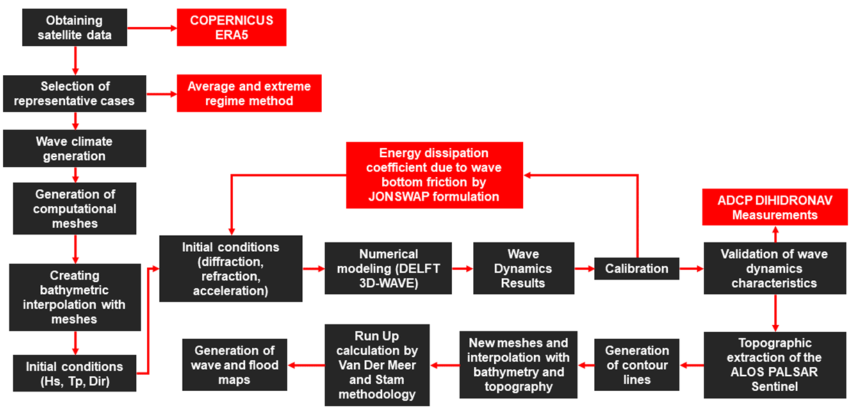


Figure 18: Numerical modeling flowchart of DELFT3D WAVE software to determine flood zones.

Based on the table shown, the range of the wave Run Up can be determined in the areas of the coast of interest.

Additionally, Figure 18 presents a numerical modeling flowchart for determining flood zones in the context of Chancay Bay. It can be noted that with the recent growth in the use of artificial intelligence, the use of predictive models of artificial neural networks (ANN), calibration and validation in a future context would be interesting to carry out. However, for the present study it would not be useful, but rather useful for training.

Below, the flood zones obtained from numerical modeling are presented, which considers the elevations of the internal coastal zone, in the maximum conditions for the south and south-southwest directions, as seen in Fig. 19 and 20.

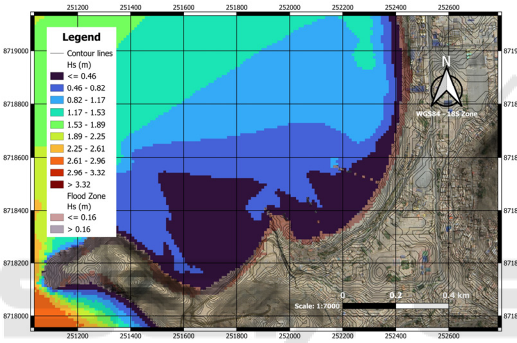


Figure 19: Flood zones in the coastal area of Chancay for the maximum condition in the south direction.

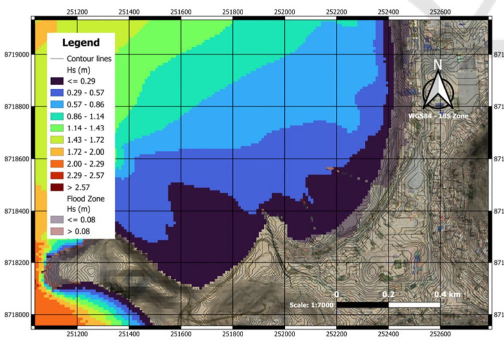


Figure 20: Flood zones in the coastal area of Chancay for the maximum condition in the south-southwest direction.

Based on Figure 19 and 20, it is determined that the range of the waves extends to levels of 4 and a maximum of 5 meters in elevation for the south direction.

The wave at points A), B) and C) of Figure 21 in a southerly direction travel between levels of 4 to 5 m, with lengths of the order of 38, 93 and 97 m up to reach wave heights of 0.15 m. That is, from the

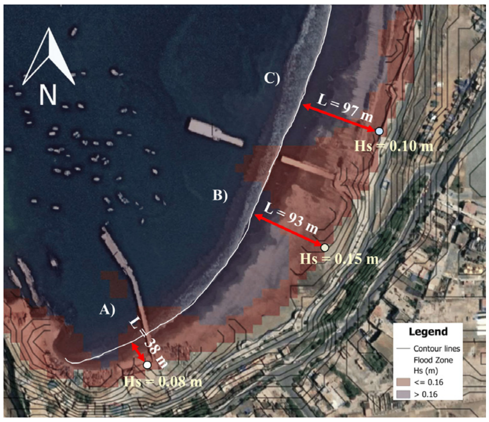


Figure 21: Flood zones with representative values for south direction.

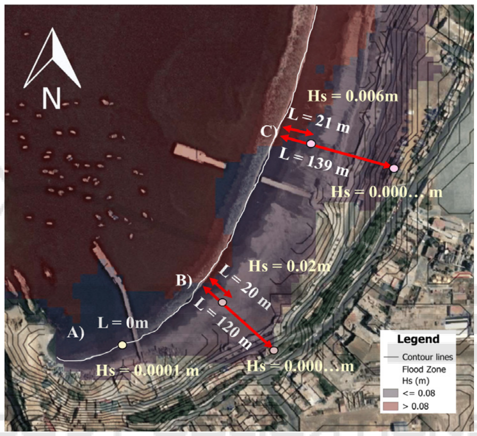


Figure 22: Flood zones with representative values for south-southwest direction.

estimated elevation of Table 9. Around 92% of it dissipated during that journey, but with great scope.

On the other hand, based on the flood zone in Figure 22 in the south-southwest direction, it is determined that the reach of the waves extends below levels of 2 m, but that they reach into the coast between the 20 and 21 m at points B) and C) with significantly low wave heights. Beyond the coast, wave heights are close to 0, which indicates that they dissipate completely beyond 3 m of terrain elevation.

Therefore, the southern direction zones contain greater relevance than the south-southwest direction due to its flooding potential due to the longitudinal reach within the coast and with wave heights of the order of 0.2 m that exceed that of the south-southwest by 96%. Therefore, an attempt at coastal protection structures, Figure 23, can be proposed in this and other stretches of the coast for future research.

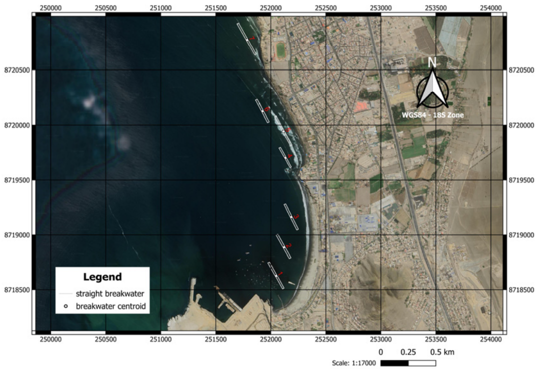


Figure 23: Tentative proposal for coastal protection structures.

## 5 VALIDATION

Based on the result of the second modeling case, calibration was performed with respect to the bottom friction coefficient of the JONSWAP formulation. This is one of the terms that condition the dissipation of wave energy, the other terms are called Whitecapping and Breaking induced by the change in depth (Alpha-Gamma). The last mentioned are limited to the proposed study, due to the scarce information on wave data.

Table 11 shows the table of bottom friction coefficient values through the iterations carried out for calibration. Then, the values are close to those measured in the field, with the southwest and south-southwest coefficients being 1.04 m2s-3 and 0.71 m2s-3, respectively. Therefore, the new calibrated and compared measurement values are as follows.

Table 11: Summary of results obtained from the calibration process of the background friction coefficient.

| Dir | Measurement | Maximum Condition | | | |
|---|---|---|---|---|---|
| | | Hs (m) | | | |
| **Bottom friction coefficient** | | **0.07** | **0.08** | **0.11** | **0.14** |
| **SW** | In Situ | 2.10 | 2.10 | 2.10 | 2.10 |
| | Delft3D | 2.92 | 2.90 | 2.87 | 2.84 |
| | **Error (%)** | **39.05** | **38.10** | **36.67** | **35.24** |
| **SSW** | In Situ | 2.10 | 2.10 | 2.10 | 2.10 |
| | Delft3D | 2.60 | 2.59 | 2.56 | 2.53 |
| | **Error (%)** | **23.81** | **23.33** | **21.90** | **20.48** |
| **Bottom friction coefficient** | | **0.19** | **0.23** | **0.29** | **0.38** |
| **SW** | In Situ | 2.10 | 2.10 | 2.10 | 2.10 |
| | Delft3D | 2.80 | 2.76 | 2.70 | 2.63 |
| | **Error (%)** | **33.33** | **31.43** | **28.57** | **25.24** |
| **SSW** | In Situ | 2.10 | 2.10 | 2.10 | 2.10 |
| | Delft3D | 2.49 | 2.45 | 2.4 | 2.33 |
| | **Error (%)** | **18.57** | **16.67** | **14.29** | **10.95** |
| **Bottom friction coefficient** | | **0.50** | **0.71** | **0.83** | **1.04** |
| **SW** | In Situ | 2.10 | 2.10 | 2.10 | 2.10 |
| | Delft3D | 2.53 | 2.36 | 2.27 | 2.13 |
| | **Error (%)** | **20.48** | **12.38** | **8.10** | **1.43** |
| **SSW** | In Situ | 2.10 | 2.10 | - | - |
| | Delft3D | 2.24 | 2.08 | - | - |
| | **Error (%)** | **6.67** | **0.95** | **-** | **-** |

Table 12: Summary of results obtained from the calibration process of the background friction coefficient.

| Dir | Measurement | Predominant Condition | | Maximum Condition | |
|---|---|---|---|---|---|
| | | Hs (m) | Tp (s) | Hs (m) | Tp (s) |
| **S** | In Situ | 1.30 | 12.60 | 2.10 | 17.30 |
| | Delft3D | 1.50 | - | 2.05 | - |
| | **Error (%)** | **15.38** | - | **2.38** | - |
| **SW** | In Situ | 1.30 | 12.60 | 2.10 | 17.30 |
| | Delft3D | 1.50 | - | 2.13 | - |
| | **Error (%)** | **15.38** | - | **1.43** | - |
| **SSW** | In Situ | 1.30 | 12.60 | 2.10 | 17.30 |
| | Delft3D | 1.42 | - | 2.08 | - |
| | **Error (%)** | **9.23** | - | **0.95** | - |

Table 12 shows how the results in maximum condition for the southwest and south-southwest directions are in the error range of 0% to 2% with respect to the ADCP measurement value.

## 6 CONCLUSIONS

The wave dynamics in Chancay Bay were studied for a period of 32 years, in which the most notable result of the research is the flood zones that put the population at risk.

To this end, modeling cases of the wave propagation of Chancay Bay were selected to determine the variational percentages with respect to the ADCP measurement from the medium regime technique to calibrate and determine the potential flooding zones of the Chancay Bay.

The results show that the flood zones reach wave heights of between 0.10 to 0.15 m, but with a large extension towards the population in the southern direction and these even exceed those in the south-southwest by 96%, thus emphasizing to the possibility of placing coastal protection structures for future research.

Finally, a large amount of data is not required to carry out the methodology suggested in this article. To carry out an investigation of this style, it is sufficient to have the bathymetry of the area through nautical charts, wave data that can be extracted from COPERNICUS ERA5 in large time series and short-term in situ wave measurements that can be used for calibration and validation of the numerical model. However, the research results can continue to be improved through information from oceanographic buoys from surrounding areas, which covers more modeling area and more robust scenarios, but with greater computational cost due to its modeling extension.

Therefore, the methodology used can be replicated in coastal areas that do not have much information on wave measurements, as is the case of the Peruvian coast and specifically the Chancay Bay as well as other parts of the world.

## REFERENCES

Wang, H., Mouche, A., Husson, R., Grouazel, A., Chapron, B., & Yang, J. (2022). Assessment of Ocean Swell Height Observations from Sentinel-1A/B Wave Mode against Buoy In Situ and Modeling Hindcasts. *Remote Sensing*, *14*(4), 862. https://doi.org/10.3390/rs14040862

Pinault, J., Morichon, D., & Roeber, V. (2020). Estimation of irregular wave runup on intermediate and reflective beaches using a phase-resolving numerical model. Journal of Marine Science and Engineering, 8(12), 1–23. https://doi.org/10.3390/jmse8120993

Prakash, N., Ashly, K. U., Seelam, J. K., Bhaskaran, H., Yadhunath, E. M., Lavanya, H. N., Krishnan, R., & Surisetty, V. V. a. K. (2021). Investigation of near-shore processes along North Goa beaches: A study based on field observations and numerical modelling. Journal of Earth System Science, 130(4). https://doi.org/10.1007/s12040-021-01755-3

Villagrán, M., Gómez, M., & Martínez, C. (2022). Coastal Erosion and a Characterization of the Morphological Dynamics of Arauco Gulf Beaches under Dominant Wave Conditions. *Water*, *15*(1), 23. https://doi.org/10.3390/w15010023

Leach, C., Hague, B. S., Kennedy, D. N., Carvalho, R. C., & Ierodiaconou, D. (2021). Identifying oceanographic conditions conducive to coastal impacts on temperate open coastal beaches. *Natural Hazards*, *109*(1), 499-521. https://doi.org/10.1007/s11069-021-04845-z

Deltares. (2023). Delft3D-WAVE User Manual, *Manuals*. Recovered from https://content.oss.deltares.nl/delft3d4/Delft3D WAVE_User_Manual.pdf [Consultation: March 28, 2023]

Ramos, C. (2017). Simulación de transporte de sedimentos en la bahía Ferrol, Chimbote. [Tesis de maestría, Universidad Nacional Mayor de San Marcos, Facultad de Ciencias Física, Unidad de Posgrado]. Repositorio institucional Cybertesis UNMSM. https://cybertesis.unmsm.edu.pe/handle/20.500.12672/6779